

Contents lists available at ScienceDirect

# Journal of Aerosol Science

journal homepage: http://www.elsevier.com/locate/jaerosci





# Size-resolved aerosol emissions from lignocellulosic biomass and biomass constituent pyrolysis under variable dilution temperatures

Luke P. McLaughlin, Erica L. Belmont

Department of Mechanical Engineering, The University of Wyoming, Laramie, WY, United States

## ARTICLE INFO

Keywords:
Biomass emissions
Aerosol
Pyrolysis
Nucleation
Agglomeration
Dilution

#### ABSTRACT

Biomass burning events produce significant amounts of particulate matter which influence global radiative forcing, decrease air quality and visibility, and have negative health impacts. The quantity, size distribution, and volatility of biomass burning aerosol emissions are influenced by the combustion mode and ensuing dilution process of the emissions mixing into ambient air. This work examined the emissions from lignocellulosic biomass and its major constituents under laboratory pyrolysis conditions to understand biomass composition and dilution temperature influences on aerosol formation. The major constituents of lignocellulosic biomass, hemicellulose (xylan), cellulose and lignin, were pyrolyzed and the resultant aerosol emissions were characterized in terms of size-resolved number and mass emission factors under variable dilution temperatures. The aerosol emissions formed from biomass constituents were then compared to those of pine and corn stover, and a summative model for predicting characteristics of biomass burning emissions from the behavior of individual constituents was assessed. Results showed a significant influence of dilution temperature on particle size, number, and distribution, with the nucleation mode of particle formation dominating. The summative model performed well in predicting particle number formation from lignocellulosic biomass, but highlighted the effect of uncertainty on predicting particle mass formation.

# 1. Introduction

Biomass burning (BB) is a multi-step process that includes heating, drying, devolatilization, and oxidation of the volatiles and char (Fang et al., 2014). BB events, such as wildland fires and prescribed fires, are significant sources of soot and organic aerosol particulate matter which affect local air quality and climate, influence global radiative forcing, and have negative health effects (Andreae & Merlet, 2001; Bond et al., 2004; Chen et al., 2017; Kuniyal & Guleria, 2019; Lokshin & Radyakin, 2012; Reid et al., 2005). Biomass burning emits about 38 Tg of PM<sub>2.5</sub> yr<sup>-1</sup> that affects local and global scales (Calvo et al., 2013), and biomass burning emissions contribute about 75% of global combustion primary organic aerosols (POA) (Bond et al., 2004). Despite anthropogenic attempts to prevent and suppress wildland fire, records suggest that the number of global fires occurring each year has increased in recent years (Cattau et al., 2020), and other studies suggest that the area burned by fires has increased in certain regions in recent decades (Gillett et al., 2004; Mouillot & Field, 2005; Westerling et al., 2006). Specifically in the Western United States (US), forests had a sharp increase

<sup>\*</sup> Corresponding author. 1000 E. University Ave, Laramie, WY, 82071, United States. *E-mail address:* ebelmont@uwyo.edu (E.L. Belmont).

in fire frequency starting in the mid-1980s with a higher frequency of large wildfires, longer wildfire durations, and longer wildfire seasons (Westerling et al., 2006). Furthermore, the climate is generally recognized as the primary fire driver, and models predict an increase in fire activity and fire impacts due to changes in the climate in future decades (Keane et al., 2015, 2004; Loehman et al., 2017, 2011; Seidl et al., 2011).

Prescribed burns are controlled biomass burning events which, like wildland fires, produce significant amounts of particulate emissions (Kobziar et al., 2015; Lee et al., 2005). Prescribed burns are the deliberate application of fire to fuels under specific conditions for the accomplishment of well-defined goals (Fernandes & Botelho, 2016), such as the reduction of fuel in a forest. Although predominantly used in the southern US, prescribed burning is used throughout the US as a land management tool (Kobziar et al., 2015) and is regulated by the Clean Air Act of 1970, as the emissions from prescribed fire can travel long distances, up to several thousand kilometers (Lee et al., 2005), influencing many communities. Nevertheless, as climate change and other anthropogenic causes increase fire frequency and severity, many have advocated for increased use of prescribed fire to manage fuel loads (Moritz et al., 2014; North et al., 2015; Schoennagel et al., 2017; Smith et al., 2016; Stephens et al., 2013).

The aerosols produced from such burning events scatter and absorb incident solar radiation, and many combustion products that are emitted to the atmosphere are reactants in atmospheric chemistry (Crutzen et al., 1985; Lobert et al., 1990; Tasoglou et al., 2017). For example, black carbon absorbs incident sunlight and heats its surroundings, thereby contributing to global warming, while other aerosols scatter incident sunlight and have a cooling effect on the earth (Engling et al., 2013; Menon et al., 2002). Besides the climate interactions, aerosols formed from biomass burning can have significant negative health effects (Chen et al., 2017; Dockery, 1994; Fowler, 2003; Lin et al., 1955; Vedal, 1997). Forest fire smoke, for example, contains a range of pollutants that can be inhaled, ingested and absorbed, and can cause a wide range of adverse effects ranging from mild eye, nose and throat irritations to persistent cardio-pulmonary conditions and even premature death (Fowler, 2003). Furthermore, polyaromatic hydrocarbons (PAHs), a product of incomplete biomass burning (Chen et al., 2017), can be in the form of volatile, semi-volatile, and particle-phase (Allen et al., 1996; Finlayson-Pitts & Pitts, 1997; Piazzalunga et al., 2013) and are carcinogenic (Kim et al., 2013; Leiter, 1942).

Biomass burning events produce significant quantities of organic aerosols (OA) (Bond et al., 2004; Hays et al., 2002) and naturally have unpredictable fire characteristics and resulting emissions, which causes significant uncertainty and difficulty in predicting and modeling the formation of POA emissions and their climate change and health impacts (Cao et al., 2019; Jolleys et al., 2014). The physical and chemical formation and evolution of biomass burning-derived OA in the atmosphere after emission is poorly understood, in part because OA exist as a metastable intermediate in the atmosphere (Chakraborty et al., 2017; Donahue et al., 2013). Because OA is composed of thousands of species with a range of temperature-dependent saturation vapor pressures, the amount of OA present in the particle form will vary with dilution, atmospheric temperature and local chemical atmosphere (May et al., 2013, 2015; Tasoglou et al., 2017; Trompetter et al., 2010). For example, studies have shown that OA produced from BB is highly volatile compared to OA derived from other sources (Cao et al., 2019; Chakraborty et al., 2017) and OA in BB plumes can increase, decrease, or remain roughly constant with time after emission depending on local conditions (Akagi et al., 2012; Capes et al., 2008; DeCarlo et al., 2008; Yokelson et al., 2009). Further complicating the prediction and modeling of OA emissions, variability within the emissions close to the source, where measurements are difficult to make, can exceed changes occurring downstream of the burning event and may represent a determining factor for biomass burning OA emissions (Jolleys et al., 2012). For example, nucleation mode particles are often present and numerous close to a biomass burning event, and nucleation mode particles transfer to accumulation mode particles as the smoke plume evolves (Engling et al., 2013; Janhäll et al., 2010; Obaidullah et al., 2018; Sippula, 2010). Furthermore, significant and dynamic transitions in the combustion phase or combustion efficiency in biomass fires correspond with changes in associated emissions profiles (Chen et al., 2007; Lee et al., 2010). The initial stages of burning significantly affect overall combustion efficiency, and the initial stages of burning can be studied via pyrolysis (Fang et al., 2014). Products of pyrolysis include permanent gases, aromatic tars, light hydrocarbons, and char, and the production of each is influenced by the ambient temperature, pressure, heating rate and biomass composition (Fang et al., 2014), where the major constituents of lignocellulosic biomass (hemicellulose, cellulose, and lignin) and the ratio of each in biomass is understood to affect tar formation and subsequent pollutant emissions during devolatilization (Chen et al.,

Due to the aforementioned complexities of biomass burning and the associated uncertainty in predicting and modeling biomass burning OA emissions, several research needs have been identified that will be addressed in this work. Particle size distributions and emission factors, particularly in terms of number emissions, have been identified as important elements in developing quantitive assessments of fire emissions because these quantities offer more granular information regarding particle dynamics and transport than overall mass-based emission factors, yet these quantities are currently seldom measured (Janhäll et al., 2010; Wardoyo et al., 2006). Additionally, the study of a broader range of fuel types, under both laboratory and ambient conditions, has been identified as necessary to more accurately ascertain the influence of fuel type and combustion process in fire emissions, specifically OA emissions (Chakraborty et al., 2017; Jolleys et al., 2014). Lastly, influential to the design of this study, there is a need for emissions experiments and inventories to report not only emission factors, but also OA concentration, temperature, and mixing state at which the emission factor was measured in order to account for and better understand gas/particle partitioning (Cao et al., 2019).

In this study, the influence of fuel composition and dilution temperature on resulting aerosol size distributions, number emission factors, and mass emission factors was characterized for the pyrolysis of the major constituents of biomass (hemicellulose, cellulose, and lignin) and lignocellulosic biomass in a laboratory setting. A thermodenuder was used to assess the volatility of these emissions. Fuel pyrolysis and emissions analysis were performed in a controlled laboratory setting to obtain new insights into the mechanisms of POA formation in naturally occurring biomass burning events. The aerosols formed from the individual constituents during pyrolysis were then compared to aerosols formed from two lignocellulosic biomasses to assess a proposed summative model to predict lignocellulosic biomass emissions from measurement of constituent-derived aerosols and the mass fraction of each constituent in the

lignocellulosic biomass.

#### 2. Methods

# 2.1. Pyrolysis and aerosol sampling

Fig. 1 is a schematic of the pyrolysis and aerosol sampling facility used in this study. The biomass constituents and lignocellulosic biomasses were pyrolyzed using a TA Instruments Q500 Thermogravimetric Analyzer (TGA) fitted with an evolved gas analysis (EGA) furnace and  $100~\mu L$  alumina sample pans. The EGA furnace is quartz-lined and thus inert to devolatilization products of the sample in order to enable accurate analysis of those products. Purge and balance gases were both ultra-high purity nitrogen ( $N_2$ , 99.999%) and were introduced to the EGA at flow rates of 90 mL/min and 10 mL/min, respectively. Temperature measurement within the EGA furnace was achieved via a K-type thermocouple adjacent to the biomass sample and was calibrated using a Curie point calibration.

Each biomass and biomass constituent sample was heated to  $100\,^{\circ}$ C in  $N_2$  and held isothermal for 10 min to dry the sample. Next, the sample was pyrolyzed by heating to  $600\,^{\circ}$ C at  $20\,^{\circ}$ C/min and held isothermal for approximately 60 min until sample mass loss and aerosol formation ceased. Starting sample sizes were approximately 0.5 mg to keep aerosol concentrations within the measurement range of the impactor and prevent saturation of the impactor electrometers. During pyrolysis, all products from the EGA furnace, emitted at a flow rate of 0.1 SLPM, were rapidly mixed with preheated air at temperatures of 22, 45, 100, and 120  $^{\circ}$ C. Dilution tests were performed with air and  $N_2$  to compare the effect of each dilution gas on the resulting aerosol numbers and distributions, and no difference was observed between the two gases so air was used for convenience. The dilution air had a fixed flow rate of  $6.7\pm0.2$  SLPM, which resulted in a dilution ratio of  $1.67\pm2$ . Although higher dilution ratios are expected to occur in the atmosphere, variation of the dilution ratio was not the focus of this study and this dilution ratio was selected to represent near-burning event conditions. The diluted aerosol stream was then drawn by a vacuum pump through a  $1.5\,$ m sample line heated to the dilution air temperature, giving the samples an approximately  $1.1\,$ s residence time over all dilution temperatures, to a Dekati High-Temperature Electrical Low-Pressure Impactor (HT-ELPI) for real-time aerosol size and number measurements. The heated sample line and particle impactor were maintained at the dilution temperature during each test to prevent further cooling of the sample after dilution and to allow for investigation of the effects of dilution temperature on primary aerosol formation. Three replicates were performed for each sample at each dilution temperature and uncertainty was assessed using the Student's t-test with a 95% confidence interval.

Several verifications were performed to ensure that the aerosols detected during experiments were not artifacts of the experimental technique, and included zero-air checks, blank sample runs, and HEPA filter tests. A zero air pump located within the HT-ELPI was used to pump filtered air through the instrument to adjust the measured current for the electrometers' bias current and zero the system before performing aerosol sampling experiments. Additionally, a blank sample was run by exposing an empty TGA sample pan to the same heating conditions as in pyrolysis experiments to quantify the contribution of background particles to the sample signals prior to running pyrolysis experiments, and these contributions were found to be negligible. To verify that measured emissions were formed upstream of the HT-ELPI and were not an artifact of the charges present in the HT-ELPI, tests were conducted with a HEPA capsule filter with a filter efficiency of 99.99% at  $0.1 \,\mu m$  added into the aerosol sampling line downstream of the dilution location and upstream of the heated line and impactor. The pyrolysis test matrix was repeated with the HEPA filter in place and results confirmed that all particles measured without the HEPA filter in place were removed.

Following the quantification of aerosol number, number size distribution and emission factors from pyrolysis of biomass and biomass constituents, the volatile fractions of measured aerosols were assessed using a thermodenuder to determine if any refractory carbon was present. A Dekati Thermodenuder TD3 was added into the aerosol sampling line downstream of the dilution location and heated line and upstream of the impactor. The pyrolysis test matrix was repeated with the thermodenuder in place for each biomass and biomass constituent and each dilution temperature, with the thermodenuder operating at 300 °C.

#### 2.2. Biomass and constituent samples and preparation

Avicel (Sigma Aldrich, PH-101), xylan (Sigma Aldrich, from Beechwood), and kraft lignin (Storaenso, from Pine and Nordic Spruce)

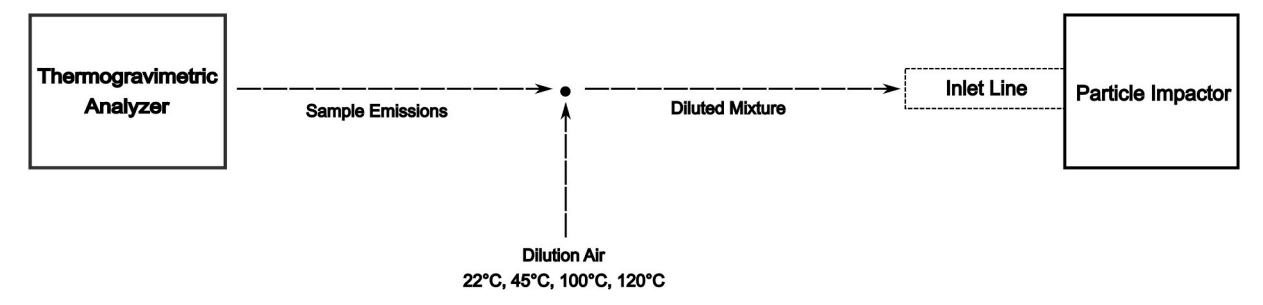


**Fig. 1.** Schematic of pyrolysis and aerosol sampling facility, including a TA Instruments Q500 Thermogravimetric Analyzer (TGA) coupled to a Dekati HT-ELPI particle impactor for aerosol characterization. Sample emissions from the TGA are mixed with dilution air at 22, 45, 100 or 120 °C. The inlet line to the particle impactor is a heated line or thermodenuder, depending on the investigation.

with a 97% dry lignin content were tested in this study as representatives of cellulose, hemicellulose, and lignin, respectively. Lodgepole pinewood collected from the Medicine Bow National Forest near Centennial, WY and corn stover collected from a farm near Scottsbluff, NE were chosen as lignocellulosic biomasses. Lignocellulosic biomasses were ground and sieved to a particle diameter range of 75–106 µm and dried for 24 h at 100 °C following sieving and prior to use in experiments. Each biomass constituent and lignocellulosic biomass sample were characterized via a modified ASTM D7582 proximate analysis method, also known as the KAR procedure (López-García et al., 2013), to determine the volatile, fixed carbon and ash contents (VC, FC, and AC, respectively) of the samples investigated in this work. The dry basis proximate analysis results, including uncertainty derived from three replicates, are shown in Table 1. The lignocellulosic biomass samples were also analyzed for constituent composition by the National Renewable Energy Lab (NREL) in Golden, CO to determine the hemicellulose, cellulose, and lignin contents of the lignocellulosic biomasses, and the results are also shown in Table 1. Galactan, arabinan, and mannan constituents of each biomass were added to the hemicellulose mass fractions of each biomass. Other constituents not included under hemicellulose, cellulose and lignin included inorganic content, which is not expected to be aerosol producing, as well as small quantities of proteins and extractives.

# 2.3. Size distributions and emission factors

As particles pass through the cascade impactor of the HT-ELPI, the charge carried by the particles is directly measured as a signal in femto-amperes and related to real-time measurement of particle number concentration. The measured particle number concentration is then related to a number emission factor,  $EF_{N_{\Delta_i}}$ , which is the number of particles collected by an individual impactor stage over a given time period and normalized by the fuel starting mass. The number emission factor of an individual stage and combined stages are defined as

$$EF_{N_{\Delta t}} = \sum_{i=1}^{n} EF_{N_{\Delta t_i}} = \sum_{i=1}^{n} \frac{C_{\Delta t_i} \cdot \dot{V} \cdot \Delta t}{m_{fuel}}$$

$$\tag{1}$$

where  $C_{\Delta t_i}$  is the time-weighted number concentration collected by stage i over time period  $\Delta t$ ,  $\dot{V}$  is the volumetric flow rate of the impactor,  $m_{fuel}$  is the starting fuel sample mass and n is the total number of stages in the HT-ELPI. The mass emission factor of each stage and combined stages are readily determined from the corresponding number emission factors and aerodynamic diameters as

$$EF_{M_{\Delta t}} = \sum_{i=1}^{n} EF_{M_{\Delta t_i}} = \sum_{i=1}^{n} \rho \cdot V_i \cdot EF_{N_{\Delta t_i}}$$
(2)

where  $\rho$  is the particle density (assumed to be 1 g·cm<sup>-3</sup> because the aerodynamic diameter is used to determine mass) and  $V_i$  is the particle volume corresponding to the aerodynamic diameter  $D_i$  of the particle. The size-resolved and total number and mass emission factors reported in this work were measured over the duration of each pyrolysis experiment.

Next, simulated pyrolysis emission factors were deduced from measured emission factors using a summative model in which the size-resolved and total emissions from each biomass constituent during pyrolysis were combined using superposition along with the corresponding mass fractions of each constituent in the biomass type to be modeled. The simulated size-resolved and total number and mass emission factors for the duration of a pyrolysis experiment were determined by

$$EF_{N_{sim}} = EF_{N_h}Y_h + EF_{N_c}Y_c + EF_{N_l}Y_l \tag{3}$$

$$EF_{M\to\infty} = EF_{Mh}Y_h + EF_{Mc}Y_c + EF_{Ml}Y_l$$
 (4)

where  $EF_{Nh}$ ,  $EF_{Nc}$ ,  $EF_{Mh}$ ,  $EF_{Mc}$ , and  $EF_{Ml}$  are the size-resolved or total number and mass emission factors determined for hemicellulose, cellulose, and lignin over the duration of the constituent pyrolysis tests.  $Y_h$ ,  $Y_c$ , and  $Y_l$  are the mass fractions of hemicellulose, cellulose, and lignin, respectively, determined for each biomass investigated in this study (Table 1).

# 2.4. Uncertainty analysis

Signal noise arising in instrument measurements causes uncertainty in the measurement and can propagate through ensuing calculations. Here, the relative error induced in calculated emission factors from biomass pyrolysis experiments due to signal noise in

**Table 1**Proximate and constituent analyses of the lignocellulosic biomass samples and major biomass constituents on a dry basis. Constituent analysis was performed by NREL.

	VC (wt%)	FC (wt%)	AC (wt%)	Lignin (wt%)	Cellulose (wt%)	Hemicellulose (wt%)
Lodgepole pine	$85.58\pm1.14$	$11.10\pm1.08$	$3.32 \pm 0.26$	28.30	35.76	20.73
Corn stover	$73.56\pm3.12$	$9.79 \pm 1.33$	$16.65\pm2.19$	12.81	28.54	22.29
Cellulose	$94.80\pm0.24$	$4.46\pm0.32$	$0.74\pm0.08$	n/a	100.0	n/a
Hemicellulose	$77.44 \pm 0.43$	$19.32\pm0.14$	$3.24\pm0.30$	n/a	n/a	100.0
Lignin	$64.66\pm0.70$	$33.70\pm1.22$	$1.64 \pm 0.53$	100.0	n/a	n/a

cascade impactor stages was determined, and the signal uncertainty was combined with the uncertainty associated with trial-to-trial deviations. The uncertainty in the number emission factor due to signal noise was determined by propagation of uncertainty applied to Eqn. (1) as

$$U_{EF_{N_{\Delta I_{i}}}} = \sqrt{\left(\frac{\partial EF_{N_{\Delta I_{i}}}}{\partial C_{\Delta I_{i}}}U_{C_{\Delta I_{i}}}\right)^{2} + \left(\frac{\partial EF_{N_{\Delta I_{i}}}}{\partial \dot{V}}U_{\dot{V}}\right)^{2} + \Delta\left(\frac{\partial EF_{N_{\Delta I_{i}}}}{\partial \Delta t}U_{\Delta t}\right)^{2} + \left(\frac{\partial EF_{N_{\Delta I_{i}}}}{\partial m_{fuel}}U_{m_{fuel}}\right)^{2}}$$
(5)

where  $U_{C_{\Delta t_i}}$ , the uncertainty in the number concentration of stage i due to signal noise measured over  $\Delta t$ , was the only uncertainty that significantly contributed to the uncertainty in the number emission factor. The uncertainty in the number concentration due to signal noise was determined by

$$U_{C_{\Delta t_i}} = \left(\frac{C_{\Delta t_i}}{S_{\Delta t_i}}\right) U_{S_{\Delta t_i}} \tag{6}$$

where  $S_{\Delta t_i}$  is the mean signal of stage i and  $U_{S_i}$  is the corresponding standard deviation of the signal, determined over the time  $\Delta t$ . Similarly, the uncertainty in the mass emission factor due to signal noise was determined by

$$U_{EF_{M_{\Delta t_{i}}}} = \sqrt{\left(\frac{\partial EF_{M_{\Delta t_{i}}}}{\partial EF_{N_{\Delta t_{i}}}} U_{EF_{N_{\Delta t_{i}}}}\right)^{2} + \left(\frac{\partial EF_{M_{\Delta t_{i}}}}{\partial V_{i}} U_{V_{i}}\right)^{2} + \left(\frac{\partial EF_{M_{\Delta t_{i}}}}{\partial \rho} U_{\rho}\right)^{2}}$$

$$(7)$$

where the uncertainty in the number emission factor due to signal noise was the only uncertainty that significantly contributed to the uncertainty in the mass emission factor. Next, the relative uncertainties in the number and mass emission factors of each stage due to signal noise were determined from the peak aerosol formation event, which corresponded with the time in the test having the largest signal uncertainty, as

$$\%U_{\Delta t_i} = \frac{U_{EF_{N_{\Delta t_i}}}}{EF_{N_{\Delta t_i}}} * 100 = \frac{U_{EF_{M_{\Delta t_i}}}}{EF_{M_{\Delta t_i}}} * 100$$
(8)

To assess the error induced by the signal noise of each stage on the total emission factors, the contribution of each stage's signal noise to the total number and mass emission factor errors for an entire pyrolysis test were determined as

$$\%E_{EF_{N_{test_i}}} = \frac{\%U_i \cdot EF_{N_{test_i}}}{EF_{N_{test}}} *100$$
(9)

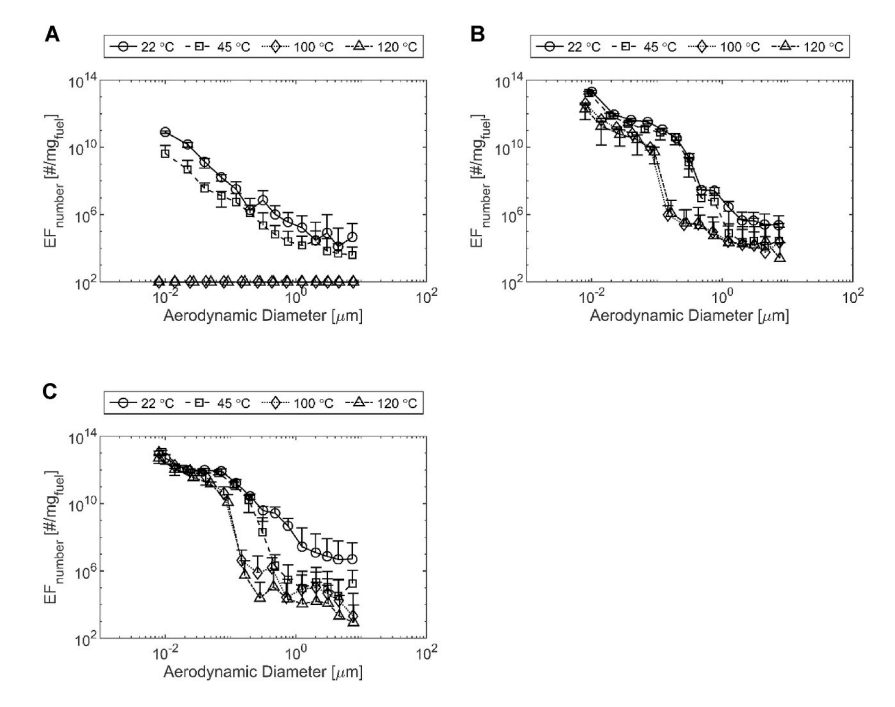


Fig. 2. Size-resolved number emission factors for a) hemicellulose, b) cellulose, and c) lignin at dilution temperatures of 22, 45, 100 and 120 °C.

$$\%E_{EF_{M_{test_i}}} = \frac{\%U_i \cdot EF_{M_{test_i}}}{EF_M} * 100 \tag{10}$$

Stages with signal noise contributing greater than 15% error to the total number and mass emission factor errors were removed from analysis to eliminate data with excessive uncertainty, and eliminated stages are clearly identified and discussed in the presented results. The 15% error criterion was selected with the aid of visual inspection of impactor collection plates and raw impactor signals following experimentation. Channels that exhibited errors averaging 15% or greater were not observed to contain any particle artifacts on the corresponding collection plate nor sensical impactor signal data, so this was deemed the critical cut-off for this study. The full data sets, including size-resolved and total number and mass emission factors for all samples, have been tabulated and are available in the Supplemental Material. Trial-to-trial uncertainty of each stage was determined using a Student's t-test with a 95% confidence interval, and signal and trial-to-trial uncertainty were combined to obtain the total uncertainty in the emission factors measured for each stage and over the entire pyrolysis test.

## 3. Results and discussion

#### 3.1. Lignocellulosic biomass constituent aerosol emission factors

Size-resolved number emission factors resulting from pyrolysis of lignocellulosic biomass constituents were determined at dilution temperatures of 22, 45, 100 and 120 °C and results are shown in Fig. 2. The highest number emission factor was observed in the smallest aerodynamic diameter bin for each sample at each dilution temperature, suggesting the majority of formed aerosols were in the nucleation mode (Janhäll et al., 2010; Obaidullah et al., 2018; Sippula, 2010). These small particles are formed by rapid quenching upon dilution of the pyrolysis emissions, inducing a gas-to-particle transition. The ensuing sample residence time in the heated line, prior to the impactor, then allows for agglomeration and growth of the volatile and semi-volatile aerosols (Janhäll et al., 2010; Obaidullah et al., 2018; Sippula, 2010). The largest number emission factor associated with each sample, except for lignin, occurred at a dilution temperature of 22 °C, with the associated aerodynamic bin size being the smallest bin size at 10 nm. The largest number emission factor was expected to occur at a dilution temperature of 22 °C because the corresponding low saturation pressure, the partial pressure beyond which condensation occurs at a temperature, was expected to induce a greater gas-to-particle transition of pyrolysis products compared to the higher saturation pressures at higher dilution temperatures. The largest number emission factor for lignin occurred in the smallest aerodynamic bin size at a dilution temperature of 45 °C; however, the number emission factor remained statistically constant at each dilution temperature, suggesting that the lignin pyrolysis products had achieved a maximum gas-to-particle conversion at each temperature in the temperature range of 22-120 °C. The number of particles found in the Aitken mode and accumulation mode (Rissler et al., 2006) decreased with increased dilution temperature for each constituent sample, and the result is attributed to less favorable particle growth at elevated temperatures, particularly exemplified by lignin (Fig. 2c) and decreased numbers of nucleation mode particles available for agglomeration and growth at elevated dilution temperatures.

Fig. 3 shows the total number emission factors of each biomass constituent sample as a function of dilution temperature, which

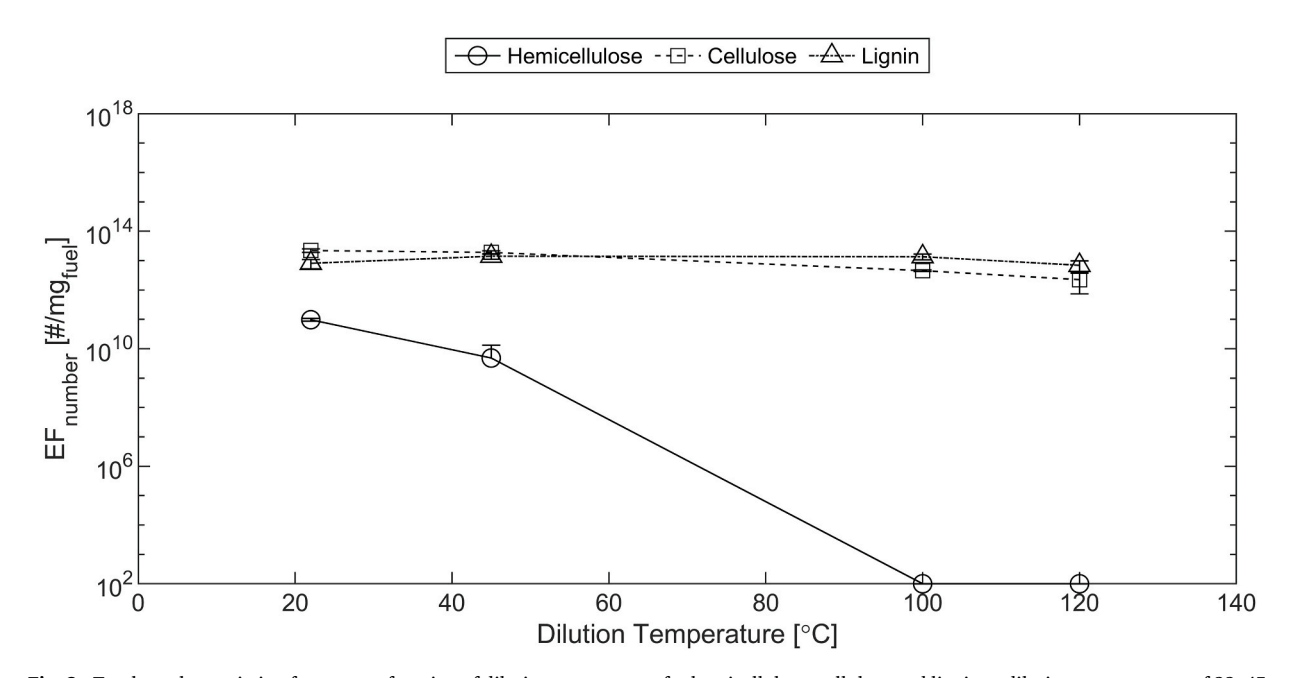


**Fig. 3.** Total number emission factors as a function of dilution temperature for hemicellulose, cellulose and lignin at dilution temperatures of 22, 45, 100 and 120 °C. Error bars represent instrument uncertainty and repeatability and are on average 33% of the measured value.

corresponds to the summation of the size-resolved number emission factors for each sample at each dilution temperature. Hemicellulose and cellulose total number emission factors decreased with increased dilution temperature, whereas lignin total number emission factor remained approximately constant with dilution temperature. The constant total number emission factor exhibited by lignin again suggests that the gas-to-particle partitioning of lignin pyrolysis products is insensitive to temperature between 22 and 120 °C because the total number of particles formed by lignin during pyrolysis is dominated by the nucleation mode particles at each dilution temperature and it is understood that the nucleation mode particles are created during a gas-to-particle transition (Sippula, 2010). Among the biomass constituent samples, cellulose and lignin produced the greatest number of particles at each dilution temperature, up to an order of 10<sup>13</sup> per mg of fuel, while hemicellulose produced significantly fewer emissions, up to an order of 10<sup>10</sup> per mg of fuel. The lower aerosol emissions of hemicellulose as well as the temperature dependence of the emissions is attributed to the pyrolysis products of hemicellulose being more prominent in the gas phase and the hemicellulose pyrolysis products having lower molecular weights and boiling points compared to the pyrolysis products of cellulose and lignin.

Figs. 4 and 5 show size-resolved mass emission factor distributions and total mass emission factors, respectively, resulting from pyrolysis of lignocellulosic biomass constituents and the aforementioned dilution temperatures. Particle size bins greater than 480 nm, 1240 nm and 480 nm for hemicellulose, cellulose, and lignin, respectively, were not included in the results of Figs. 4 and 5 because their signal uncertainty contributed excessive uncertainty to the total mass emission factor per the criteria set in this study. The significant uncertainty in mass emission factors at large particle sizes elucidates the cubic effect of uncertainty propagation when translating from number to mass emission factors.

Size-resolved mass emission factor distributions (Fig. 4) show that peak mass emission factors occurred in aerodynamic bin sizes of 22 nm, 200 nm, and 72 nm for hemicellulose, cellulose, and lignin, respectively. The mass emission factor distribution is observed to be markedly different than the number emission factor distribution for each constituent sample, respectively, highlighting the dominating effect larger particles have on the mass distribution of emissions and the relatively low mass representation of nucleation mode particles, despite nucleation mode particles dominating the number emission factor.

The total mass emission factors (Fig. 5) were largest at a dilution temperature of 22 °C for each constituent sample, and the total mass emission factors decreased with increased dilution temperature for each constituent sample. Among the constituents, lignin produced the largest total mass emission factor at each dilution temperature and had a maximum mass emission factor of nearly 0.65 mg/mg<sub>fuel</sub> at a dilution temperature of 22 °C. Cellulose also produced a significant amount of emissions, producing an emission factor of nearly 0.40 mg/mg<sub>fuel</sub> at a dilution temperature of 22 °C. Hemicellulose, however, produced near negligible mass emission factors at each dilution temperature and is therefore expected to contribute relatively little to the aerosol mass formation from pyrolysis of native lignocellulosic biomasses. It should be noted that the particle mass emission factors determined in the biomass constituents are large compared to those reported for typical biomass burning, such as emission factors by Hays et al. for the Pinaceae family burning (11.2–33.5 g/kg) (Hays et al., 2002) and by Janhäll et al. for burning forests (9.6  $\pm$  4.6 g/kg), savannas (6.3  $\pm$  3.0 g/kg) and grass lands (4.7  $\pm$  2.1 g/kg) (Janhäll et al., 2010). Such a discrepancy arises due to the nature of the pyrolysis experiments performed herein where particle precursor species are not oxidized prior to particle formation, and the concentration of pyrolysis products having the same saturation pressure is far greater for a pure lignocellulose biomass constituent than those measured from a lignocellulosic biomass,

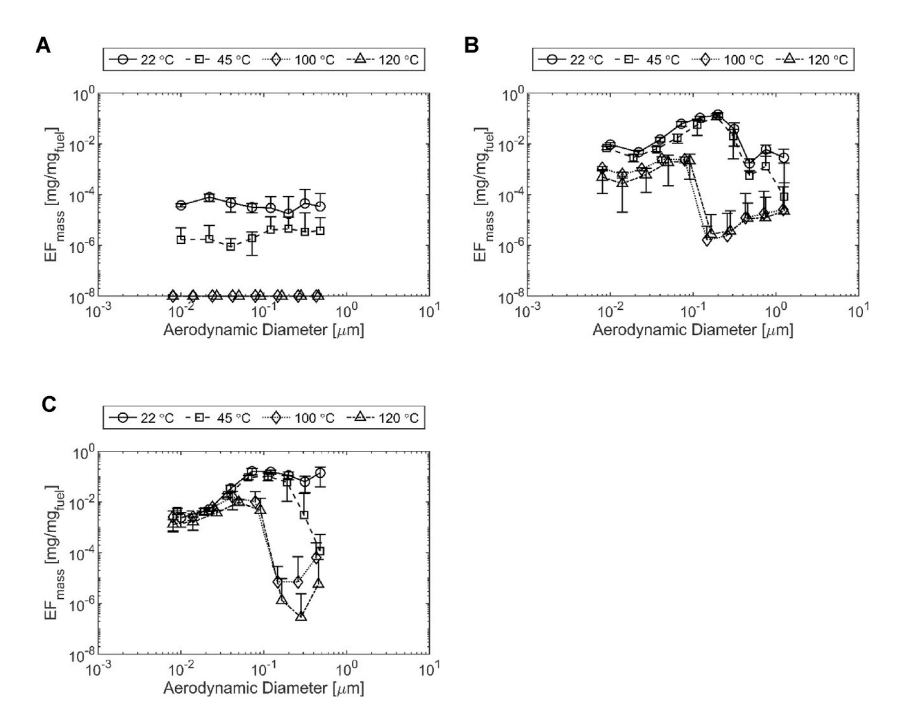


Fig. 4. Size-resolved mass emission factors for a) hemicellulose, b) cellulose, and c) lignin at dilution temperatures of 22, 45, 100 and 120 °C.

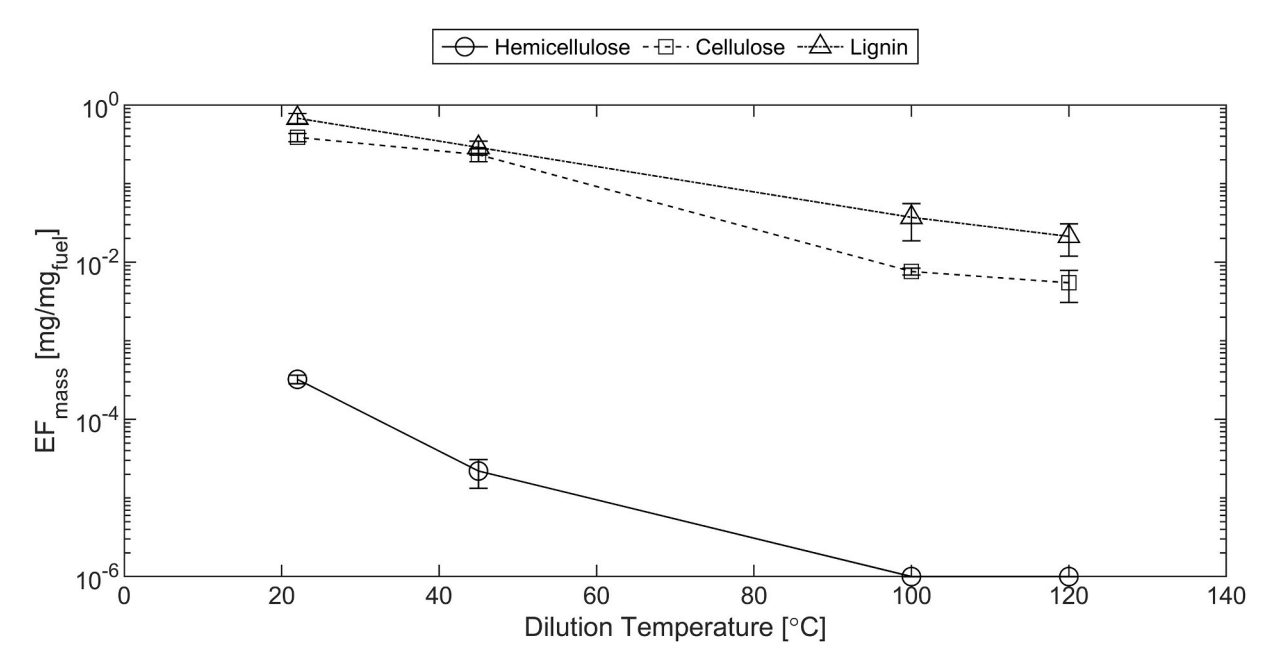


Fig. 5. Total mass emission factors as a function of dilution temperature for hemicellulose, cellulose and lignin at dilution temperatures of 22, 45, 100 and 120 °C. Error bars represent instrument uncertainty and repeatability and are on average 23% of the measured value.

causing a greater conversion from gas to particle. Furthermore, the concentration of pyrolysis products was relatively large in these experiments compared to dilution of emissions into the atmosphere or large environments and it is understood that a higher concentration of particle precursor gases results in a larger gas to particle conversion (May et al., 2013).

# 3.2. Measured and simulated lignocellulosic biomass aerosol emission factors

Following analysis of biomass constituent emissions, pine and corn stover emissions were analyzed at variable dilution temperatures and the summative emissions model developed in this work was evaluated. Simulated pine and corn stover aerosol emissions were predicted using individual constituent data for hemicellulose, cellulose, and lignin (Figs. 2–5), along with the constituent analysis performed by NREL (Table 1). Fig. 6 shows the total number emission factor comparison between measured and simulated pine (Fig. 6a) and measured and simulated corn stover (Fig. 6b), each as a function of dilution temperature. The total number emission factors for pine decreased with increased dilution temperature, and the measured and simulated emissions showed very good quantitative agreement with an average deviation of 17% at each dilution temperature. Similarly, the total number emission factors for corn stover decreased with increased dilution temperature, and an average deviation of 176% between measured observations and simulated emissions was observed at each dilution temperature.

Pine produced a greater total number emission factor at each dilution temperature when compared to corn stover. Based upon the individual constituent number emissions (Figs. 2 and 3), the larger number emission factor of the pine compared to the corn stover is partly attributed to the pine and corn stover having approximately similar amounts of cellulose, but the pine having a greater quantity of lignin compared to the corn stover (Table 1). Cellulose and lignin were found in this work to produce the highest number emissions per unit mass among the lignocellulosic biomass constituents, making them major contributors to early-stage pyrolysis aerosol

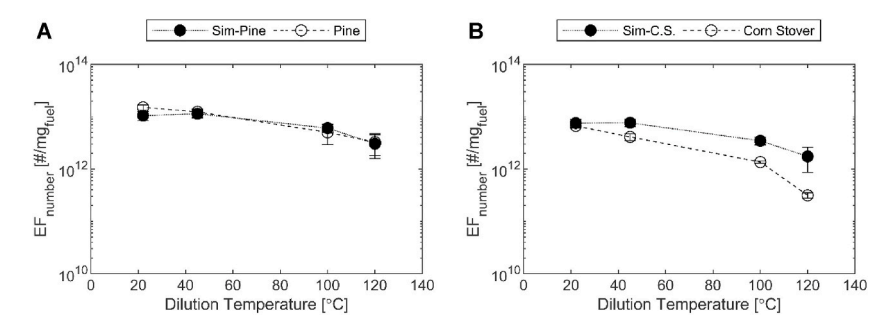


Fig. 6. Comparison of a) measured and simulated pine total number emission factors, and b) measured and simulated corn stover total number emission factors, each as functions of dilution temperature.

## formation.

Figs. 7 and 8 show particle size distributions for the total number emission factors presented in Fig. 6 for pine (Fig. 7) and corn stover (Fig. 8). Again, reasonable agreement was observed between the simulated and measured biomass results in each aerodynamic size bin at each dilution temperature for both biomass samples, with average deviations of up to one order of magnitude between simulated and measured emissions for both pine and corn stover.

Fig. 9 shows the total mass emission factors of measured and simulated pine and corn stover as functions of dilution temperature. Bin sizes greater than 1240 nm were removed from the total mass emission factor analysis due to excessive uncertainty at these larger bin sizes. Similar to the number emission factors, the simulated and measured total mass emission factors of pine and corn stover decreased with increased dilution temperature, and the quantities of the measured and simulated emissions agreed within an average deviation of 153% and 807% at each dilution temperature for pine and corn stover, respectively. Larger discrepancies between measured and simulated total mass emission factors were observed as compared with measured and simulated total number emission factors (Fig. 6), again highlighting the cubic effect of uncertainty propagation when translating from number to mass emission factors. These observations further strengthen the need for inclusion of number emissions data in atmospheric climate models (Andreae & Rosenfeld, 2008; Fuzzi et al., 2011; Lohmann et al., 2007). Comparing the two native biomasses, pine produced a larger total mass emission factor at each dilution temperature compared to corn stover. Similar to the total number emission factor, the increased aerosol mass formed from pine pyrolysis is attributed, in part, to its additional lignin content compared to corn stover. These results align with the hypothesis that forest fire particles are on average larger than particles formed by savanna and grass fires (Janhäll et al., 2010); despite the experiments here having been performed on a much smaller scale with fewer factors influencing emissions, the production of more nucleation mode particles from pine measured in this study would lead to the larger particles measured in field studies due to the associated increased agglomeration also observed in this study.

Figs. 10 and 11 give size-resolved distribution details of the discrepancies between the simulated and measured mass emissions for pine (Fig. 10) and corn stover (Fig. 11). The disagreement between measured and simulated results was most pronounced at the two lowest dilution temperatures for pine, where the simulated mass emissions exceeded measurements by an order of magnitude at both 22 °C and 45 °C. Simulated corn stover emissions exceeded measured values by up to two orders of magnitude at each dilution temperature; however, agreement within one order of magnitude or better in many size bins was observed. Results suggest that the agglomeration mechanism is more pronounced for the individual constituents than for the native biomass samples, as observed by the overprediction of mass in the simulated pine and corn stover bins ≥70 nm when compared to the native pine and corn stover, respectively. The discrepancy between the experiments and summative model suggests that there is enhanced interaction between the individual constituent pyrolysis products during the nucleation and agglomeration processes following pyrolysis and emissions dilution, which may be due to higher concentrations of the volatile and semi-volatile species emitted from pure constituents (May et al., 2013).

Overall, the summative model predicted well the trend and size distributions of aerosol emissions formed from lignocellulosic biomass pyrolysis and the impacts of dilution temperature. The size-resolved number emission factors were overpredicted by the

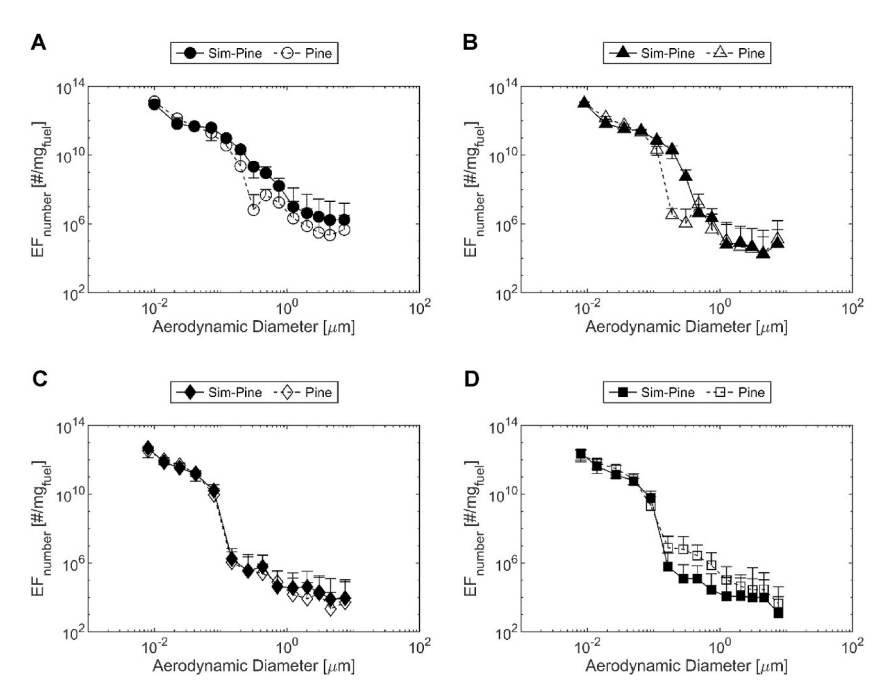


Fig. 7. Comparison of size-resolved number emission factors for measured and simulated pine at dilution temperatures of a) 22  $^{\circ}$ C, b) 45  $^{\circ}$ C, c) 100  $^{\circ}$ C and d) 120  $^{\circ}$ C.

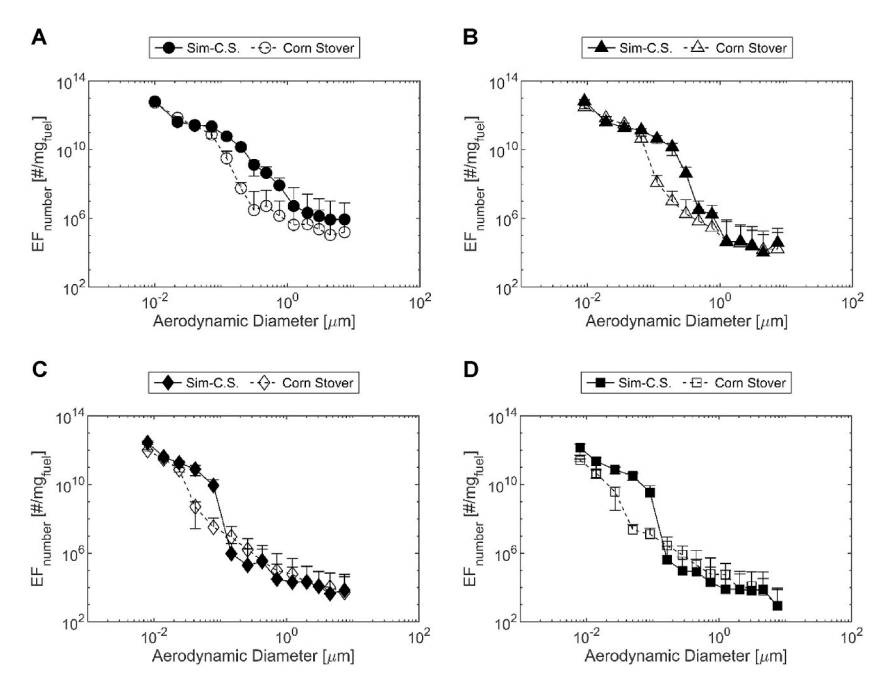


Fig. 8. Comparison of size-resolved number emission factors for measured and simulated corm stover at dilution temperatures of a) 22  $^{\circ}$ C, b) 45  $^{\circ}$ C, c) 100  $^{\circ}$ C and d) 120  $^{\circ}$ C.

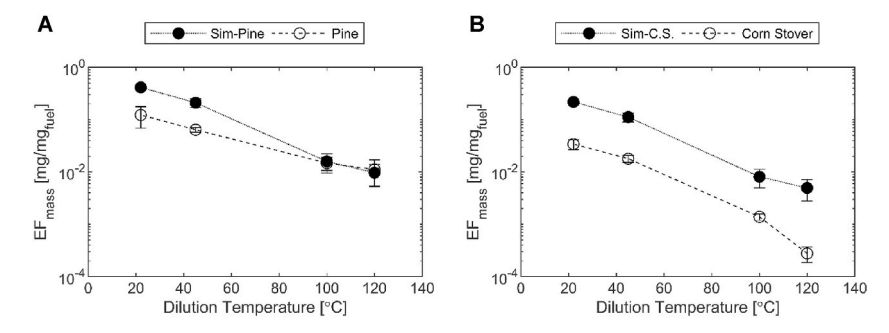


Fig. 9. Comparison of a) measured and simulated pine total mass emission factors and b) measured and simulated corn stover total mass emission factor, each as functions of dilution temperature.

summative model at larger particle sizes due to enhanced agglomeration observed for constituent pyrolysis, which was not as pronounced in the measured biomass emissions. This discrepancy did not significantly impact total number emission factors, however, due to the significantly higher number of nucleation mode particles. The total and size-resolved mass emissions were less successfully captured as compared to number emissions, however, due to the significant aerosol mass associated with the larger, agglomeration-mode particles. Thus, the enhanced agglomeration, apparent in the discrepancies between the summative model and measured total mass emission factors (Fig. 9), is not apparent in the summative model-derived total number emissions factors (Fig. 6). The summative model results, as well as the significant uncertainty in mass emission factors at large particle sizes, further highlight the cubic effect of uncertainty propagation when translating from number to mass emission factors.

In assessing the success of the model, it should also be recognized that the lignocellulosic biomass constituent representatives used in this work had somewhat different structures than those in native biomass (Qu et al., 2011). Cellulose composition and pyrolysis products are consistent among various crystalline celluloses extracted from different biomass sources; however, compositions and pyrolysis products are understood to vary for hemicellulose and lignin extracted from different biomasses (Buranov & Mazza, 2008; Qu et al., 2011). Moreover, lignin pyrolysis product distributions are understood to vary greatly from species to species and even within the same biomass family, such as softwoods, hardwoods and grasses (Buranov & Mazza, 2008; Wang et al., 2009). Here, the simulated and measured pine number emission factors agreed well while simulated corn stover number emission factors overpredicted the emissions for the native corn stover. This discrepancy is likely contributed to by the lignin constituent used in this work, which was sourced from pine wood, not corn stover, as lignin of herbaceous crops is understood to vary structurally compared to softwoods and hardwoods (Buranov & Mazza, 2008). Specifically, lignin derived from woody biomasses contain mainly guaiacyl and syringyl units,

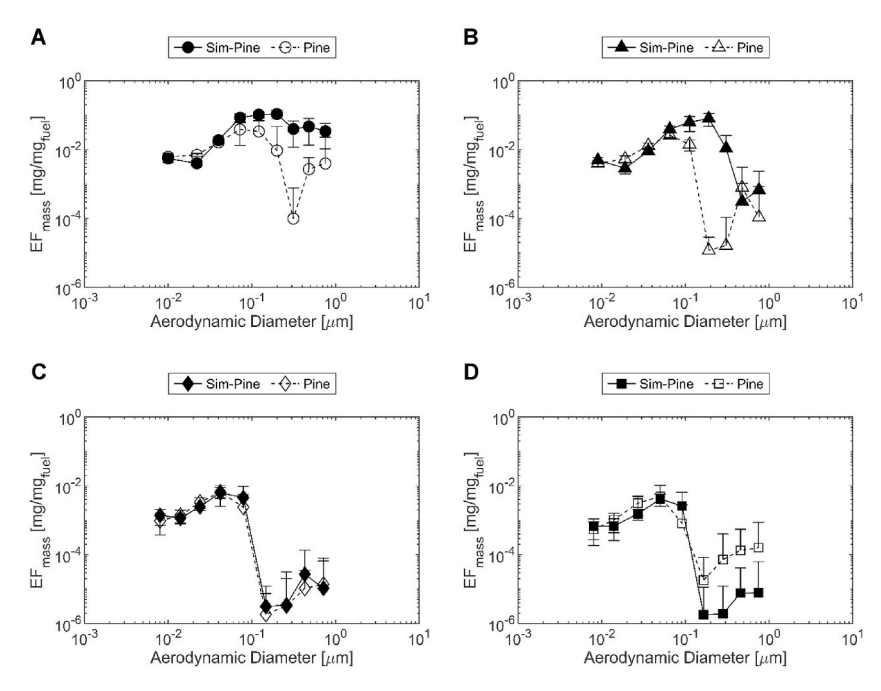


Fig. 10. Comparison of measured and simulated pine mass emission factor size distributions at dilution temperatures of a)  $22 \,^{\circ}$ C, b)  $45 \,^{\circ}$ C, c)  $100 \,^{\circ}$ C and d)  $120 \,^{\circ}$ C.

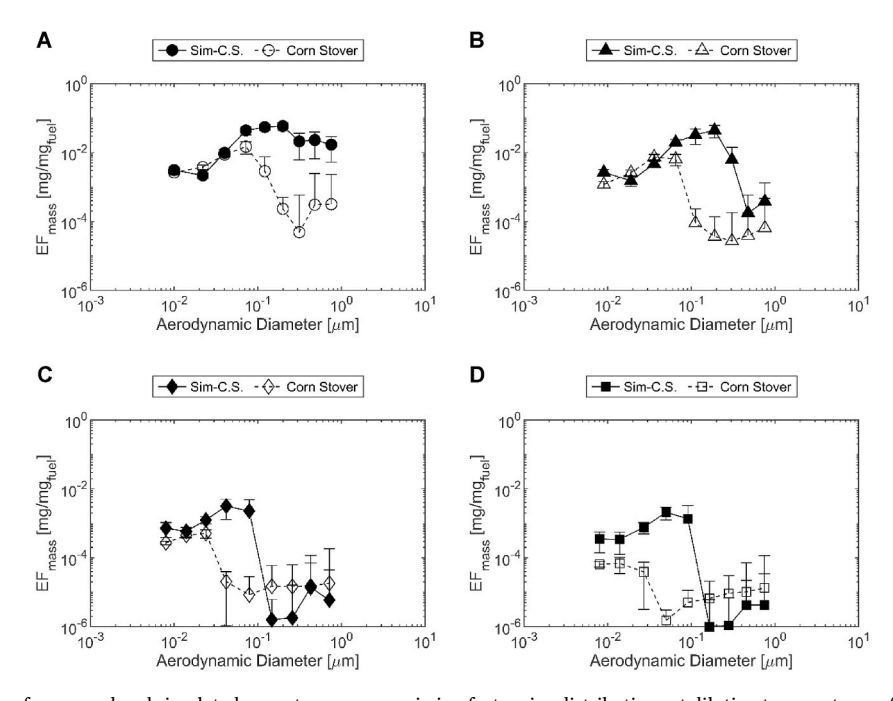


Fig. 11. Comparison of measured and simulated corn stover mass emission factor size distributions at dilution temperatures of a)  $22 \,^{\circ}$ C, b)  $45 \,^{\circ}$ C, c)  $100 \,^{\circ}$ C and d)  $120 \,^{\circ}$ C.

whereas the lignin derived from herbaceous plants contain guaiacyl, syringyl, and *p*-hydroxyphenyl units in significant amounts with different ratios (Billa et al., 1998; Buranov & Mazza, 2008).

# 3.3. Volatility investigation

The volatility of aerosol emissions formed from pyrolysis of biomass constituents and native biomasses was assessed using a

thermodenuder, and aerosols were found to be completely removed from the sample stream when the thermodenuder was operated at 300 °C. While a more granular assessment of aerosol volatility (Grieshop et al., 2009; Saleh et al., 2012) was outside the scope of this work, this finding indicates that all of the aerosols produced during pyrolysis in this study were semi-volatile and volatile (Grieshop et al., 2009; Huffman et al., 2009; Liang et al., 1998; May et al., 2013). Specifically, this indicates an absence of refractory carbon and other high molecular weight compounds in the aerosol emissions. This result, in addition to the sensitivity of the number and size of emissions to dilution temperature, reflects the sensitivity of biomass pyrolysis aerosol formation to ambient conditions and provides insights into the dynamic gas/particle partitioning process of biomass pyrolysis aerosols following the pyrolysis event.

#### 4. Conclusions

The major constituents of lignocellulosic biomass (hemicellulose, cellulose and lignin) were pyrolyzed and the resultant aerosol emissions were characterized in terms of particle size and quantity under variable dilution temperatures and at a fixed dilution ratio and rate. The aerosol emissions formed from the biomass constituents were compared to those of native biomasses, specifically pine and corn stover, and a summative model for predicting characteristics of biomass pyrolysis emissions from biomass composition and measured emissions from individual biomass constituents was assessed. Results showed a significant influence of dilution temperature on particle size, number, and distribution, with the nucleation mode of particle formation dominating at each dilution temperature investigated here, and number and mass emissions were observed to increase with decreasing dilution temperature. The summative model performed well in predicting the trend of both number and mass emissions with dilution temperature, and also performed well in quantitatively predicting the total number formation from lignocellulosic biomass, particularly pine. The effect of uncertainty on quantitative prediction of particle mass formation, however, was highlighted. The importance of selecting proper biomass constituent representatives was also identified for a summative model approach. The findings of this work provide a building block towards a fundamental approach to prediction of aerosol emissions from biomass pyrolysis and burning.

# Declaration of competing interest

The authors declare that they have no known competing financial interests or personal relationships that could have appeared to influence the work reported in this paper.

## Acknowledgments

The contributions of Dr. Ed Wolfrum from the National Renewable Energy Laboratory (NREL) in Golden, CO to this work are gratefully acknowledged here.

# Appendix A. Supplementary data

Supplementary data to this article can be found online at https://doi.org/10.1016/j.jaerosci.2020.105679.

# **Funding sources**

This work was supported by the National Science Foundation Graduate Research Fellowship Award #1650114 and the National Science Foundation Award #1847498.

# References

- Akagi, S. K., Craven, J. S., Taylor, J. W., McMeeking, G. R., Yokelson, R. J., Burling, I. R., et al. (2012). Evolution of trace gases and particles emitted by a chaparral fire in California. Atmospheric Chemistry and Physics, 12(3), 1397–1421. https://doi.org/10.5194/acp-12-1397-2012
- Allen, J. O., Dookeran, N. M., Smith, K. A., Sarofim, A. F., Taghizadeh, K., & Lafleur, A. L. (1996). Measurement of polycyclic aromatic hydrocarbons associated with size-segregated atmospheric aerosols in Massachusetts. *Environmental Science and Technology*, 30(3), 1023–1031. https://doi.org/10.1021/es9505170
- Andreae, M. O., & Merlet, P. (2001). Emission of trace gases and aerosols from biomass burning. Global Biogeochemical Cycles, 15(4), 955–966. https://doi.org/
- Andreae, M. O., & Rosenfeld, D. (2008). Aerosol-cloud-precipitation interactions. Part 1. The nature and sources of cloud-active aerosols. *Earth-Science Reviews*, 89 (1–2), 13–41. https://doi.org/10.1016/j.earscirev.2008.03.001
- Billa, E., Koukios, E. G., & Monties, B. (1998). Investigation of lignins structure in cereal crops by chemical degradation methods. *Polymer Degradation and Stability*, 59 (1–3), 71–75. https://doi.org/10.1016/s0141-3910(97)00152-3
- Bond, T. C., Streets, D. G., Yarber, K. F., Nelson, S. M., Woo, J. H., & Klimont, Z. (2004). A technology-based global inventory of black and organic carbon emissions from combustion. *Journal of Geophysical Research: Atmosphere*, 109(14), 1–43. https://doi.org/10.1029/2003JD003697
- Buranov, A. U., & Mazza, G. (2008). Lignin in straw of herbaceous crops. Industrial Crops and Products, 28(3), 237–259. https://doi.org/10.1016/j.
- Calvo, A. I., Alves, C., Castro, A., Pont, V., Vicente, A. M., & Fraile, R. (2013). Research on aerosol sources and chemical composition: Past, current and emerging issues. Atmospheric Research, 120–121, 1–28. https://doi.org/10.1016/j.atmosres.2012.09.021
- Cao, L. M., Huang, X. F., Wang, C., Zhu, Q., & He, L. Y. (2019). Characterization of submicron aerosol volatility in the regional atmosphere in Southern China. Chemosphere, 236, 124383. https://doi.org/10.1016/j.chemosphere.2019.124383

- Capes, G., Johnson, B., McFiggans, G., Williams, P. I., Haywood, J., & Coe, H. (2008). Aging of biomass burning aerosols over West Africa: Aircraft measurements of chemical composition, microphysical properties, and emission ratios. *Journal of Geophysical Research Atmospheres*, 113(23), 1–13. https://doi.org/10.1029/2008.ID009845
- Cattau, M. E., Wessman, C., Mahood, A., & Balch, J. K. (2020). Anthropogenic and lightning-started fires are becoming larger and more frequent over a longer season length in the U.S.A. Global Ecology and Biogeography, 29(4), 668–681. https://doi.org/10.1111/geb.13058
- Chakraborty, A., Tripathi, S. N., & Gupta, T. (2017). Effects of organic aerosol loading and fog processing on organic aerosol volatility. *Journal of Aerosol Science, 105* (January 2016), 73–83. https://doi.org/10.1016/j.jaerosci.2016.11.015
- Chen, Y., Charpenay, S., Jensen, A., Wójtowicz, M. A., & Serio, M. A. (1998). Modeling of biomass pyrolysis kinetics. Symposium (International) on Combustion, 27(1), 1327–1334. https://doi.org/10.1016/S0082-0784(98)80537-7
- Chen, J., Li, C., Ristovski, Z., Milic, A., Gu, Y., Islam, M. S., et al. (2017). A review of biomass burning: Emissions and impacts on air quality, health and climate in China. *The Science of the Total Environment, 579*(November 2016), 1000–1034. https://doi.org/10.1016/j.scitotenv.2016.11.025
- Chen, L. W. A., Moosmüller, H., Arnott, W. P., Chow, J. C., Watson, J. G., Susott, R. A., et al. (2007). Emissions from laboratory combustion of wildland fuels: Emission factors and source profiles. Environmental Science and Technology, 41(12), 4317–4325. https://doi.org/10.1021/es062364i
- Crutzen, P. J., Delany, A. C., Greenberg, J., Haagenson, P., Heidt, L., Lueb, R., et al. (1985). Tropospheric chemical composition measurements in Brazil during the dry season. *Journal of Atmospheric Chemistry*, 2(3), 233–256. https://doi.org/10.1007/BF00051075
- DeCarlo, P. F., Dunlea, E. J., Kimmel, J. R., Aiken, A. C., Sueper, D., Crounse, J., et al. (2008). Fast airborne aerosol size and chemistry measurements above Mexico City and Central Mexico during the MILAGRO campaign. Atmospheric Chemistry and Physics, 8(14), 4027–4048. https://doi.org/10.5194/acp-8-4027-2008
- Dockery, D. (1994). Acute Respiratory Effects of Particulate Air Pollution. Annual Review of Public Health, 15(1), 107–132. https://doi.org/10.1146/annurev.publhealth.15.1.107
- Donahue, N. M., Chuang, W., Epstein, S. A., Kroll, J. H., Worsnop, D. R., Robinson, A. L., Adams, P. J., & Pandis, S. N. (2013). Why do organic aerosols exist? Understanding aerosol lifetimes using the two-dimensional volatility basis set. *Environmental Chemistry*, 10(3), 151–157. https://doi.org/10.1071/EN13022
- Engling, G., Lee, J. J., Sie, H. J., Wu, Y. C., & I, Y. P. (2013). Anhydrosugar characteristics in biomass smoke aerosol-case study of environmental influence on particle-size of rice straw burning aerosol. *Journal of Aerosol Science*, 56, 2–14. https://doi.org/10.1016/j.jaerosci.2012.10.001
- Fang, J., Leavey, A., & Biswas, P. (2014). Controlled studies on aerosol formation during biomass pyrolysis in a flat flame reactor. Fuel, 116, 350–357. https://doi.org/10.1016/j.fuel.2013.08.002
- Fernandes, P., & Botelho, H. S. (2016). A review of prescribed burning effectiveness in fire hazard reduction. *International Journal of Wildland Fire*, 117–128. https://doi.org/10.1071/WF02042. January 2003.
- Finlayson-Pitts, B. J., & Pitts, J. N. (1997). Tropospheric air pollution: Ozone, airborne toxics, polycyclic aromatic hydrocarbons, and particles. *Science*, 276(5315), 1045–1052. https://doi.org/10.1126/science.276.5315.1045
- Fowler, C. (2003). Human Health Impacts of Forest Fires in the Southern United States: A Literature Review. Journal of Ecological Anthropology, 7(1), 39–63. https://doi.org/10.5038/2162-4593.7.1.3
- Fuzzi, S., Andreae, M. O., Huebert, B. J., Kulmala, M., Bond, T. C., Boy, M., et al. (2011). Critical assessment of the current state of scientific knowledge, terminology, and research needs concerning the role of organic aerosols in the atmosphere, climate, and global change. *Atmospheric Chemistry and Physics*, 15(3), 12–19. https://doi.org/10.3929/ethz-a-010782581
- Gillett, N. P., Weaver, A. J., Zwiers, F. W., & Flannigan, M. D. (2004). Detecting the effect of climate change on Canadian forest fires. *Geophysical Research Letters*, 31 (18). https://doi.org/10.1029/2004GL020876
- Grieshop, A. P., Miracolo, M. A., Donahue, N. M., & Robinson, A. L. (2009). Constraining the volatility distribution and gas-particle partitioning of combustion aerosols using isothermal dilution and thermodenuder measurements. *Environmental Science and Technology*, 43(13), 4750–4756. https://doi.org/10.1021/
- Hays, M. D., Geron, C. D., Linna, K. J., Smith, N. D., & Schauer, J. J. (2002). Speciation of Gas-Phase and Fine Particle Emissions from Burning of Foliar Fuels. Environmental Science and Technology, 36(11), 2281–2295. https://doi.org/10.1021/es0111683
- Huffman, J. A., Docherty, K. S., Mohr, C., Cubison, M. J., Ulbrich, I. M., Ziemann, P. J., et al. (2009). Chemically-resolved volatility measurements of organic aerosol from different sources. *Environmental Science and Technology*, 43(14), 5351–5357. https://doi.org/10.1021/es803539d
- Janhäll, S., Andreae, M. O., & Pöschl, U. (2010). Biomass burning aerosol emissions from vegetation fires: particle number and mass emission factors and size distributions. *Atmospheric Chemistry and Physics*, 10(3), 1427–1439. https://doi.org/10.5194/acp-10-1427-2010
- Jolleys, M. D., Coe, H., McFiggans, G., Capes, G., Allan, J. D., Crosier, J., et al. (2012). Characterizing the aging of biomass burning organic aerosol by use of mixing ratios: A meta-analysis of four regions. *Environmental Science and Technology*, 46(24), 13093–13102. https://doi.org/10.1021/es302386v
- Jolleys, M. D., Coe, H., McFiggans, G., McMeeking, G. R., Lee, T., Kreidenweis, S. M., Jr., et al. (2014). Organic aerosol emission ratios from the laboratory combustion of biomass fuels. *Journal of Geophysical Research: Atmosphere*, 850–871. https://doi.org/10.1002/2014JD021589
- Keane, R. E., Cary, G. J., Davies, I. D., Flannigan, M. D., Gardner, R. H., Lavorel, S., et al. (2004). A classification of landscape fire succession models: Spatial simulations of fire and vegetation dynamics. *Ecological Modelling*, 179(1–2), 3–27. https://doi.org/10.1016/j.ecolmodel.2004.03.015
- Keane, R. E., McKenzie, D., Falk, D. A., Smithwick, E. A. H., Miller, C., & Kellogg, L. K. B. (2015). Representing climate, disturbance, and vegetation interactions in landscape models. *Ecological Modelling*, 309(310), 33–47. https://doi.org/10.1016/j.ecolmodel.2015.04.009
- Kim, K. H., Jahan, S. A., Kabir, E., & Brown, R. J. C. (2013). A review of airborne polycyclic aromatic hydrocarbons (PAHs) and their human health effects. Environment International, 60, 71–80. https://doi.org/10.1016/j.envint.2013.07.019
- Kobziar, L. N., Godwin, D., Taylor, L., & Watts, A. C. (2015). Perspectives on trends, effectiveness, and impediments to prescribed burning in the southern. *U.S. Forests*, 6(3), 561–580. https://doi.org/10.3390/f6030561
- Kuniyal, J. C., & Guleria, R. P. (2019). The current state of aerosol-radiation interactions: A mini review. *Journal of Aerosol Science*, 130, 45–54. https://doi.org/10.1016/j.jaerosci.2018.12.010. July 2018.
- Lee, S., Baumann, K., Schauer, J. J., Sheesley, R. J., Naeher, L. P., Meinardi, S., et al. (2005). Gaseous and particulate emissions from prescribed burning in Georgia. Environmental Science and Technology, 39(23), 9049–9056. https://doi.org/10.1021/es0515831
- Lee, T., Sullivan, A. P., MacK, L., Jimenez, J. L., Kreidenweis, S. M., Onasch, T. B., Worsnop, D. R., Malm, W., Wold, C. E., Hao, W. M., & Collett, J. L. (2010). Chemical smoke marker emissions during flaming and smoldering phases of laboratory open burning of wildland fuels. *Aerosol Science and Technology*, 44(9). https://doi.org/10.1080/02786826.2010.499884
- Leiter, J. (1942). Production of subcutaneous sarcomas in mice with tars extracted from atmospheric dusts. *Journal of the National Cancer Institute*, 3(2), 155–165. https://doi.org/10.1093/inci/3.2.155
- Liang, C., Pankow, J. F., Odum, J. R., & Seinfeld, J. H. (1998). Gas/particle partitioning of semivolatile organic compounds to model inorganic, organic, and ambient smog aerosols. *Environmental Science and Technology*, 31(11), 3086–3092. https://doi.org/10.1021/es9702529
- Lin, Y., Ma, Y., Qiu, X., Li, R., Fang, Y., Wang, J., Zhu, Y., & Hu, D. (1955). Sources, transformation, and health implications of PAHsand their nitrated, hydroxylated, and oxygenatedderivatives in PM2.5in Beijing. *Nature*, 175(4449), 238. https://doi.org/10.1038/175238c0
- Lobert, J. M., Scharffe, D. H., Hao, W. M., & Crutzen, P. J. (1990). Importance of biomass burning in the atmospheric budgets of nitrogen-containing gases. *Nature*, 346 (6284), 552–554. https://doi.org/10.1038/346552a0
- Loehman, R. A., Clark, J. A., & Keane, R. E. (2011). Modeling effects of climate change and fire management on western white pine (Pinus monticola) in the Northern Rocky Mountains, USA. Forests, 2(4), 832–860. https://doi.org/10.3390/f2040832
- Loehman, R. A., Keane, R. E., Holsinger, L. M., & Wu, Z. (2017). Interactions of landscape disturbances and climate change dictate ecological pattern and process: spatial modeling of wildfire, insect, and disease dynamics under future climates. *Landscape Ecology*, 32(7), 1447–1459. https://doi.org/10.1007/s10980-016-0414-6
- Lohmann, U., Stier, P., Hoose, C., Ferrachat, S., Kloster, S., Roeckner, E., et al. (2007). Cloud microphysics and aerosol indirect effects in the global climate model ECHAM5-HAM. Atmospheric Chemistry and Physics, 7(13), 3425–3446. https://doi.org/10.5194/acp-7-3425-2007

- Lokshin, M., & Radyakin, S. (2012). Month of birth and children's health in India. *Journal of Human Resources*, 47(1), 174–203. https://doi.org/10.3368/jhr.47.1.174
  López-García, M., Lodeiro, P., Herrero, R., Barriada, J. L., Rey-Castro, C., David, C., et al. (2013). Experimental evidences for a new model in the description of the adsorption-coupled reduction of Cr(VI) by protonated banana skin. *Bioresource Technology*, 139, 181–189. https://doi.org/10.1016/j.biortech.2013.04.044
- May, A. A., Lee, T., McMeeking, G. R., Akagi, S., Sullivan, A. P., Urbanski, S., et al. (2015). Observations and analysis of organic aerosol evolution in some prescribed fire smoke plumes. *Atmospheric Chemistry and Physics*, 15(11), 6323–6335. https://doi.org/10.5194/acp-15-6323-2015
- May, A. A., Levin, E. J. T., Hennigan, C. J., Riipinen, I., Lee, T., Collett, J. L., et al. (2013). Gas-particle partitioning of primary organic aerosol emissions: 3. Biomass burning. Journal of Geophysical Research Atmospheres, 118(19), 11,327–11,338, https://doi.org/10.1002/jgrd.50828
- Menon, S., Hansen, J., Nazarenko, L., & Luo, Y. (2002). Climate effects of black carbon aerosols in China and India. Science, 297(5590), 2250–2253. https://doi.org/10.1126/science.1075159
- Moritz, M. A., Batllori, E., Bradstock, R. A., Gill, A. M., Handmer, J., Hessburg, P. F., et al. (2014). Learning to coexist with wildfire. *Nature*, 515(7525), 58–66. https://doi.org/10.1038/nature13946
- Mouillot, F., & Field, C. B. (2005). Fire history and the global carbon budget: A  $1^{\circ} \times 1^{\circ}$  fire history reconstruction for the 20th century. Global Change Biology, 11(3), 398–420. https://doi.org/10.1111/j.1365-2486.2005.00920.x
- North, B. M. P., Stephens, S. L., Collins, B. M., Agee, J. K., Aplet, G., Franklin, J. F., et al. (2015). Reform forest fire management: Agency incentives undermine policy effectiveness. *Science*, 6254, 1280–1281. https://doi.org/10.1126/science.aab2356
- Obaidullah, M., Bram, S., & Ruyck, J. De (2018). An Overview of PM Formation Mechanisms from Residential Biomass Combustion and Instruments Using in PM Measurements. *International Journal of Energy and Environment*, 12(May), 41–50. ISSN: 2308-1007.
- Piazzalunga, A., Anzano, M., Collina, E., Lasagni, M., Lollobrigida, F., Pannocchia, A., et al. (2013). Contribution of wood combustion to PAH and PCDD/F concentrations in two urban sites in Northern Italy. *Journal of Aerosol Science*, 56, 30–40. https://doi.org/10.1016/j.jaerosci.2012.07.005
- Qu, T., Guo, W., Shen, L., Xiao, J., & Zhao, K. (2011). Experimental study of biomass pyrolysis based on three major components: Hemicellulose, cellulose, and lignin. Industrial & Engineering Chemistry Research, 50(18), 10424–10433. https://doi.org/10.1021/ie1025453
- Reid, J. S., Koppmann, R., Eck, T. F., Eleuterio, D. P., Division, M., Juelich, F., et al. (2005). A review of biomass burning emissions part II: intensive physical properties of biomass burning particles. *Atmospheric Chemistry and Physics*, 5, 799–825. https://doi.org/10.5194/acp-5-799-2005
- Rissler, J., Vestin, A., Swietlicki, E., Fisch, G., Zhou, J., Artaxo, P., et al. (2006). Size distribution and hygroscopic properties of aerosol particles from dry-season biomass burning in Amazonia. Atmospheric Chemistry and Physics, 6(2), 471–491. https://doi.org/10.5194/acp-6-471-2006
- Saleh, R., Khlystov, A., & Shihadeh, A. (2012). Determination of evaporation coefficients of ambient and laboratory-generated semivolatile organic aerosols from phase equilibration kinetics in a thermodenuder. *Aerosol Science and Technology*, 46(1), 22–30. https://doi.org/10.1080/02786826.2011.602762
- Schoennagel, T., Balch, J. K., Brenkert-Smith, H., Dennison, P. E., Harvey, B. J., Krawchuk, M. A., et al. (2017). Adapt tomore wildfire in western North American forests as climate changes. *Proceedings of the National Academy of Sciences of the United States of America*, 114(18), 4582–4590. https://doi.org/10.1073/pnas.1617464114
- Seidl, R., Fernandes, P. M., Fonseca, T. F., Gillet, F., Jönsson, A. M., Merganičová, K., et al. (2011). Modelling natural disturbances in forest ecosystems: A review. Ecological Modelling, 222(4), 903–924. https://doi.org/10.1016/j.ecolmodel.2010.09.040
- Sippula, O. (2010). Fine Particle Formation and Emissions in Biomass Combustion. In Report series in aerosol science (Vol. 108). http://www.atm.helsinki.fi/FAAR/. Helsinki 2010.
- Smith, A. M. S., Kolden, C. A., Paveglio, T. B., Cochrane, M. A., Bowman, D. M. J. S., Moritz, M. A., et al. (2016). The Science of Firescapes: Achieving Fire-Resilient Communities. *BioScience*, 66(2), 130–146. https://doi.org/10.1093/biosci/biv182
- Stephens, S. L., Agee, J. K., Fulé, P. Z., North, M. P., Romme, W. H., Swetnam, T. W., et al. (2013). Managing forests and fire in changing climates. *Science*, 342 (October), 41–42. https://doi.org/10.1126/science.1240294
- Tasoglou, A., Saliba, G., Subramanian, R., & Pandis, S. N. (2017). Absorption of chemically aged biomass burning carbonaceous aerosol. *Journal of Aerosol Science, 113* (August), 141–152. https://doi.org/10.1016/j.jaerosci.2017.07.011
- Trompetter, W. J., Davy, P. K., & Markwitz, A. (2010). Influence of environmental conditions on carbonaceous particle concentrations within New Zealand. *Journal of Aerosol Science*, 41(1), 134–142. https://doi.org/10.1016/j.jaerosci.2009.11.003
- Vedal, S. (1997). Ambient Particles and Health: Lines that Divide. Journal of the Air and Waste Management Association, 47(5), 551–581. https://doi.org/10.1080/10473289.1997.10463922
- Wang, S., Wang, K., Liu, Q., Gu, Y., Luo, Z., Cen, K., et al. (2009). Comparison of the pyrolysis behavior of lignins from different tree species. *Biotechnology Advances*, 27(5), 562–567. https://doi.org/10.1016/j.biotechadv.2009.04.010
- Wardoyo, A. Y. P., Morawska, L., Ristovski, Z. D., & Marsh, J. (2006). Quantification of particle number and mass emission factors from combustion of Queensland trees. *Environmental Science and Technology*, 40(18), 5696–5703. https://doi.org/10.1021/es0609497
- Westerling, A. L., Hidalgo, H. G., Cayan, D. R., & Swetnam, T. W. (2006). Warming and earlier spring increase Western U.S. forest wildfire activity. Science, 313(5789), 940–943. https://doi.org/10.1126/science.1128834
- Yokelson, R. J., Crounse, J. D., DeCarlo, P. F., Karl, T., Urbanski, S., Atlas, E., et al. (2009). Emissions from biomass burning in the Yucatan. Atmospheric Chemistry and Physics, 9(15), 5785–5812. https://doi.org/10.5194/acp-9-5785-2009